MHD electroosmotic micro-pump of non-Newtonian fluids through micro-channel

M. Abdulhameed

[a]*School of Science and Technology*
The Federal Polytechnic, Bauchi,
P.M.B. 0231, Off Dass Road, Bauchi, Nigeria

Abstract

This problem deals with steady driven pressure flow and heat transfer of electro-magneto-hydrodynamic micro-pump of third grade fluids between two micro-parallel plates embedded in a porous medium. The effect of thermal radiation and electro-kinetic have been taken into account. The flow forced by the Lorentz force, produced by the interaction of a vertical magnetic field and an externally horizontal imposed electrical field, is assumed to be unidirectional and one dimensional. Based upon the velocity field, the thermally fully developed heat transfer with radiation effect are analyzed by taking the viscous dissipation, the volumetric heat generation due to Joule heating effect and electromagnetic couple effect into account. Analytical solutions corresponding to the fluid velocity and temperature distribution are obtained in series forms, in the assumption that the non-Newtonian viscoelastic parameter has small values. The effects of permeability of the porous medium K, the dimensionless electrical strength parameter H, Hartmann number Ha, non-Newtonian parameter Lamda, constant pressure P, thermal radiation Nr and non-dimensional parameter Brinkman number gamma1 on the velocity and temperature are investigated graphically and discussed in detail.

Keywords: Electro-magneto-hydrodynamic (EMHD), Micro-pump of third grade fluid, Porous microchannel, thermo-fluidic transport,

1. Introduction

Microfluidics found to be important role in many technological processes and applications, involving detection, separation and analysis of chemical and biological samples, micro-electro-mechanical systems(MEMS), and material processing and biotechnology. Transport phenomena at the micro-scale level reveal many features that are not observed in the macro-

scale devices. Mirza et al. [10] have studied the blood flow along with particles suspension through microcapillary using the electro-magneto-hydrodynamic (EMH) approach. They have obtained analytical solutions for the governing model equations analytically using the Laplace and finite Hankel transforms. Results showed that the motion of blood and particles are controlled by regulating the electrokinetic and magnetic parameters. Sinha et al. [13] have presented a vivid theoretical study on heat transfer feature together with fully developed EMH flow of blood through a capillary, having electrokinetic effects with emphases on constant heat flux at the wall. Effects of thermal radiation and velocity slip condition were taken into consideration. A mathematical model was developed for Joule heating in electro-osmotic flow, including the Poisson-Boltzmann equation, the momentum equation and the energy equation. Results showed that the temperature of blood can be controlled by regulating Joule heating parameter. Rokni et al. [11]have studied the effects of EMH on both nanofluid flow and heat transfer characteristics in a rotating system. The governing equations were solved using the fourth-order Runge-Kutta method. The Effects of electric, magnetic, Reynolds number and rotation parameters on skin friction coefficient and rate of heat transfer were considered. Obtained results indicated that the Nusselt number increases with an increase in the magnetic parameter, electric parameter and Reynolds number but it decreases with an increase in rotation parameter. Jian et al. [8] have analyzed the analytical solution of transient rotating EMH flow through a parallel micro-channel. Analytical inquiry for combined transient rotating of both electrically conducting incompressible and viscous fluid between two slit micro parallel plates were performed using the method of separation of variables. Comparison of theoretical results with related experimental data was performed when rotation effect is lacked. Ko et al. [9] have studied, the non-reflective boundary conditions for the EMH flow simulation. EMH model was expressed in standard form, that is in Cartesian coordinates for both with linear constitutive relations and artificial compressibility. It was found that there is a strong mutual interactions between the flow field and the electromagnetic field. Chakraborty et al. [4] have analyzed critically the characteristics of heat transfer associated with thermal developed combined EMH flows through narrow flow channels, with emphases to electrokinetics effects, for the constant wall heat flux condition. The liquid flow was activated by the combination of imposed pressure-gradient, electrokinetic effects and electromagnetic interactions. Result showed that for the development of state-of-the-art electro-magneto-mechanical devices, with improved efficiency and functionality, the

applications in the field of micro-scale thermal management were required. Zhao et al. [15] have investigated the characteristics of heat transfer of thermally developed nanofluid flow through a parallel microchannel plate under the combined influences of externally applied axial pressure gradient and transverse magnetic field.They have obtained analytical solutions for the EMH flow in the microchannels using the Debye-Huckel linearization. Results for pertinent dimensionless parameters on the velocity, temperature and Nusselt number were discussed and presented graphically. Recently, Wang et al. [14] have analyzed the problem of EMH micro-pump of third grade fluids between two micro-parallel plates. They obtained analytical solutions for the velocity and temperature using both perturbation techniques and the Chebyshev spectral collocation method. The influence of magnetic and electric fields on the velocity and temperature distribution have been analyzed.

A more general form of EMH flow and heat transfer of third-grade fluids problems can be derived when fluid porosity and thermal radiation in the micro-channel are considered. The governing model equations must be modified with an additional new term in the momentum equation and energy equation to represent respectively, the fluid porosity and radiation terms. Recently, Wang et al. [14] derived an analytical solution for the steady EMH flow of third-grade fluid and heat transfer when fluid porosity and thermal radiation in the micro-channel are not considered. They used a perturbation method combined with finite difference method to solve the governing flow and energy equations. However, the corresponding solutions of the [14] problem for the electro-magneto-hydrodynamic flow of third-grade fluid and heat transfer in a porous medium with radiation effects are not reported so far. Hence, this is the motivation of the present work.

The study of EMH flow and heat transfer through a porous medium with radiation effects has become an active area of research due to its varied applications in science and engineering. A few of these applications are found in micro-fluidic devices. These micro-scale devices are candidates for applications in heat transfer augmentation, micro-electronics and micro-electro-mechanical systems (MEMS), miniaturized chemical reactors and combustors, aerospace, and biomedical systems. The aim of this article is to extend the analysis of Wang et al. [14] in two directions. These are (i) to take into account the porous medium and (ii) to consider radiation effects. More exactly, the analytical solutions of the steady EMH flow and heat transfer of third-grade fluid in a porous medium with radiation effect using perturbation technique are presented. An important feature of this technique lies in the fact that the

approximate solutions to the fluid velocity, temperature distribution are obtained in series forms under the assumption small value of non-Newtonian viscous-elastic parameter. The rest of the paper is arranged as follows: Section 2 gives the mathematical formulation of the problem. Section 3 contains the analytical solutions for the fluid velocity and temperature distribution. In Section 4 the results are graphically presented and discussed for various parameters of physical interest, followed by the conclusions in Section 5.

2. Problem formulation

The steady fully developed flow of incompressible third-grade fluid through a rectangular microchannel in the presence of electric and magnetic fields is considered. A schematic figure of the problem, including the mechanical physics in the cartesian coordinates (x, y, z) is shown in Fig.1, where x-axis and z-axis are tangential to the charged surface and y-axis is perpendicular to the charged plates. The pressure driven flow is also driven by Lorentz force along x direction which is produced by the externally imposed electrical fields of intensity E inverse z direction and applied magnetic field of flux density B in the y direction. In the present study, the length of the porous microchannel in x-axis is L, the widthin z-axis is W and the height is $2h$ (since the typical height of the microchannel h is $100 - 200\mu m$). It is supposed that both height $2h$ and width W are much less than the length L, i.e., $2h \ll L$ and $W \ll L$ [14]. The $2D$ rectangular duct flow reduces to a $1D$ micro-parallel channel flow problem and the velocity becomes independent of the z-coordinate.

The fluid velocity of the flow is governed by continuity equation and Navier–Stokes equation:

$$\nabla \overrightarrow{u} = 0, \tag{1}$$

$$\rho \frac{\partial \overrightarrow{u}}{\partial t} = -\nabla p + \mu \nabla^2 \overrightarrow{\tau} + \overrightarrow{F}_{em}, \tag{2}$$

where ρ is the fluid density, $\overrightarrow{u}$ is the velocity field, t is the time, p is the pressure, μ is dynamic viscosity, $\overrightarrow{\tau}$ is the stress tensor and $\overrightarrow{F}_{em}$ is the net body force per unit volume acting on the fluid, which is essentially contributed by the electrical force, Lorentz force acting on the system and Darcy's resistance, can be written as:

$$\overrightarrow{F}_{em} = \overrightarrow{J} \times \overrightarrow{B} + \overrightarrow{R}, \tag{3}$$

where $\overrightarrow{B}$ is the magnetic field along the y direction and is assumed constant of magnitude B, $\overrightarrow{R}$ is the Darcy's resistance to the flow in the porous medium and $\overrightarrow{J}$ is the local ion

current density obtained from the Ohm's law in a moving frame:

$$\overrightarrow{J} = \sigma\left(\overrightarrow{E} + \overrightarrow{u} \times \overrightarrow{B}\right), \tag{4}$$

where σ is the electrical conductivity of the fluid and $\overrightarrow{E}$ is the electric field inverse z direction and assumed to be a constant E.

For third-grade fluid, the extra Cauchy stress tensor is given by [2, 12, 7, 14]:

$$\overrightarrow{\tau} = -pI + \mu\overrightarrow{A}_1 + \alpha_1\overrightarrow{A}_2 + \alpha_2\overrightarrow{A}_1^2 + \beta_1\overrightarrow{A}_3 + \beta_2\left(\overrightarrow{A}_1\overrightarrow{A}_2 + \overrightarrow{A}_2\overrightarrow{A}_1\right) + \beta_3\left(tr\overrightarrow{A}_1^2\right)\overrightarrow{A}_1, \tag{5}$$

where μ is the viscosity of the fluid and α_1, α_2, β_1, β_2,β_3 are the material constants of the third grade fluid. $\overrightarrow{A}_1$, $\overrightarrow{A}_2$ and $\overrightarrow{A}_3$ are kinematical tensors and can be expressed as

$$\overrightarrow{A}_1 = (\text{grad}\,\overrightarrow{u}) + (\text{grad}\,\overrightarrow{u})^T \tag{6}$$

$$\overrightarrow{A}_n = \frac{d\overrightarrow{A}_{n-1}}{dt} + \overrightarrow{A}_{n-1}(\text{grad}\,\overrightarrow{u}) + \overrightarrow{A}_{n-1}(\text{grad}\,\overrightarrow{u})^T\overrightarrow{A}_{n-1}, \quad n = 2, 3, ... \tag{7}$$

The Darcy's resistance can be interpreted as a measure of the resistance to the flow in the porous medium. For steady unidirectional flow over the rigid plate, the x-component expression of R_x for a third-grade fluids is given by [5, 3, 6]

$$R_x = -\frac{\phi}{K_1}\left[\mu + 2(\beta_2 + \beta_3)\left(\frac{du}{dy}\right)^2\right]u, \tag{8}$$

where ϕ is the porosity of the porous medium and .K_1 is the is the permeability of the porous medium.

The energy equation including volumetric joule heating, electromagnetic couple effect and stress tensor for viscouelastic fluid can be used to give the temperature distribution in the microchannel [8, 1, 14]

$$\rho c_p\left(\frac{\partial T}{\partial t} + \overrightarrow{u}\frac{\partial T}{\partial X}\right) = \overrightarrow{\tau} : (\text{grad}\,\overrightarrow{u}) - \nabla q + \frac{\overrightarrow{J}\overrightarrow{J}}{\sigma}. \tag{9}$$

2.1. Analytical solution of velocity field

Using the above assumption, the velocity is along x-axis and can be expressed as:

$$\overrightarrow{u} = [u(y),\ 0,\ 0] \tag{10}$$

Substituting Eqs. (3)-(8) and (10) into the momentum Eq. (2), we get:

$$\begin{aligned}\frac{dp}{dx} &= \mu\frac{d^2u}{dy^2} + 2(\beta_2 + \beta_3)\frac{d}{dy}\left[\left(\frac{du}{dy}\right)^3\right] \\ &\quad -\frac{\phi}{K_1}\left[\mu + 2(\beta_2 + \beta_3)\left(\frac{du}{dy}\right)^2\right]u - \sigma B^2 u + \sigma BE,\end{aligned} \tag{11}$$

$$\frac{dp}{dy} = 2\left(\alpha_1 + \alpha_2\right)\frac{d}{dy}\left[\left(\frac{du}{dy}\right)^2\right], \tag{12}$$

$$\frac{dp}{dz} = 0. \tag{13}$$

Considering the pressure gradient along along x-axis, Eqs. (11)-(13) reduce to following:

$$\mu\frac{d^2u}{dy^2} + 2\left(\beta_2 + \beta_3\right)\frac{d}{dy}\left[\left(\frac{du}{dy}\right)^3\right]$$
$$-\frac{\phi}{K_1}\left[\mu + 2\left(\beta_2 + \beta_3\right)\left(\frac{du}{dy}\right)^2\right]u - \sigma B^2 u + \sigma BE + \left(-\frac{dp}{dx}\right) = 0. \tag{14}$$

The boundary condition subjected to Eq. (14) is given by:

$$u\left(y\right) = 0 \qquad \text{at} \qquad y = \pm h. \tag{15}$$

Consider the following dimensionless parameters:

$$y^* = \frac{y}{h}, \quad u^* = \frac{u}{\nu/h}, \quad \Lambda = \frac{\left(\beta_2 + \beta_3\right)\nu^2}{\mu h^4}, \quad Ha = Bh\sqrt{\frac{\sigma}{\mu}}, \quad H = \frac{\sigma BEh^3}{\mu\nu}, \quad \frac{1}{K} = \frac{\phi h^2}{K_1}. \tag{16}$$

We obtained the following dimensionless problem (dropping the $*$ notation):

$$\frac{d^2u}{dy^2} + 6\Lambda\frac{d}{dy}\left[\left(\frac{du}{dy}\right)^3\right] - \frac{u}{K}\left[1 + 2\Lambda\left(\frac{du}{dy}\right)^2\right] - Ha^2u + H + P = 0 \tag{17}$$

$$u\left(y\right) = 0 \qquad \text{at} \qquad y = \pm 1, \tag{18}$$

where Ha is Hartmann number, which gives an estimate of the magnetic forces compared to the viscous forces and H is the dimensionless parameter related to the electrical strength.

In order to derive the solution by perturbation method, we assume that $0 < \Lambda \ll 1$ so that we assume the solution for velocity in the following form

$$u\left(y\right) = u_0 + \Lambda u_1 + 0\left(\Lambda^2\right). \tag{19}$$

Substitution Eq. (19) into Eqs. (17), (18) and separating at each order of Λ, we obtain the following equations and boundary conditions:

Order zero:

$$\frac{\partial^2 u_0}{\partial y^2} - \left(Ha^2 + \frac{1}{K}\right)u_0 + P + H = 0, \tag{20}$$

$$u_0\left(\pm 1\right) = 0. \tag{21}$$

Order one

$$\frac{d^2u_1}{dy^2}+6\Lambda\left(\frac{du_0}{dy}\right)^2\left(\frac{d^2u_0}{dy^2}\right)-Ha^2u_1-\frac{1}{K}\left((2u_0)\left(\frac{du_0}{dy}\right)^2+u_1\right), \tag{22}$$

$$u_1(\pm1)=0. \tag{23}$$

Now by using DSolve algorithm in a symbolic computer algebra package MATHEMATICA, the solutions of the boundary valued problems Eqs. (20)-(23) are:

$$u_0=K(H+P)\frac{\left(\cos\left[\frac{\sqrt{-1-Ha^2x}}{\sqrt{x}}\right]-\cos\left[\frac{\sqrt{-1-Ha^2xy}}{\sqrt{x}}\right]\right)\sec\left[\frac{\sqrt{-1-Ha^2x}}{\sqrt{x}}\right]}{1+Ha^2K} \tag{24}$$

$$\begin{aligned}
u_1 \;=\;& \frac{-1}{96\left(1+Ha^2K\right)^3}(K^{\frac{3}{2}}(H+P)^3\sec\left[\frac{\sqrt{-1-Ha^2K}}{\sqrt{K}}\right]^4\\
&\left\{2\sqrt{K}(14+9Ha^2K)\cos\left[\frac{\sqrt{-1-Ha^2K}}{\sqrt{K}}\right]^3\cos\left[\frac{\sqrt{-1-Ha^2K}y}{\sqrt{K}}\right]\right.\\
&\left.-32\sqrt{K}\cos\left[\frac{\sqrt{-1-Ha^2K}}{\sqrt{K}}\right]^2(3+\cos\left[\frac{2\sqrt{-1-Ha^2K}y}{\sqrt{K}}\right]\right\}\\
&+24\sqrt{-1-Ha^2K}\left(2+3Ha^2K\right)\cos\left[\frac{\sqrt{-1-Ha^2K}y}{\sqrt{K}}\right]\sin\left[\frac{\sqrt{-1-Ha^2K}}{\sqrt{K}}\right]\\
&-\cos\left[\frac{\sqrt{-1-Ha^2K}}{\sqrt{K}}\right](6\sqrt{K}(2+3Ha^2K)\cos\left[\frac{\sqrt{-1-Ha^2K}y}{\sqrt{K}}\right]^3\\
&+\sqrt{K}\cos\left[\frac{\sqrt{-1-Ha^2K}y}{\sqrt{K}}\right](-88-3(14+9Ha^2K)\cos\left[\frac{2\sqrt{-1-Ha^2K}}{\sqrt{K}}\right]\\
&+9(2+3Ha^2K)\cos\left[\frac{2\sqrt{-1-Ha^2K}y}{\sqrt{K}}\right])\\
&+24\sqrt{-1-Ha^2K}(2+3Ha^2K)y\sin\left[\frac{\sqrt{-1-Ha^2K}y}{\sqrt{K}}\right])))
\end{aligned} \tag{25}$$

It is important mentioning that when $K=0$ (non-porous medium) and $P=O$ (non-pressure gradient), Eqs. (24) and (25) reduce to those found by [14].

3. Electro-magneto-hydrodynamic heat transfer analysis

The second novelty of the present study is to delineate the thermal radiation characteristics associated with EMH flow of third-grade fluid through a micro-channel, the solution of the energy equation is integral to the present analysis. The energy equation associated with third-grade fluid with radiation effects is given by:

$$\rho c_p\left(\frac{\partial T}{\partial t}+u\frac{\partial T}{\partial X}\right)=K_{th}\frac{\partial^2T}{\partial y^2}-\frac{\partial q_y}{\partial y}+\sigma\left(E^2+B^2u^2-2EBu\right)+\mu\left(\frac{\partial u}{\partial y}\right)^2+2\left(\beta_2+\beta_3\right)\left(\frac{\partial u}{\partial y}\right)^4, \tag{26}$$

where c_p is the specific heat at constant pressure, T is the temperature, K_{th} is the thermal conductivity, q_y is the radiative heat flux.

It should be noted that in Eq. (26), the second term on the right hand side represents the contribution due to thermal radiation, the third term represents a volumetric heat generation due to Joule heating and the last two terms represent a local volumetric heating due to viscoelastic dissipation.

The boundary conditions for the energy equation are:

$$K_{th}\frac{dT}{dy} = q_s \quad \text{or} \quad T = T_s \quad \text{at} \quad y = \pm h. \tag{27}$$

The radiative heat flux according to the Rosseland approximation is given by

$$q_y = -\frac{4\sigma^*}{3K^*}\frac{\partial T^4}{\partial y}, \tag{28}$$

where σ^* is the Stefan-Boltzmann constant and k^* is the mean absorbtion coefficient. Suppose that the small variation between fluid temperature T and wall temperature T_s, T^4 can be expressed as a linear combination of the temperature. Hence, we can write T^4 in a Taylor's series expansion about T_s as follows:

$$T^4 = T_s^4 + 4T_s^3\left(T - T_s\right) + 6T_s^2\left(T - T_s\right)^2 + ... \tag{29}$$

Neglecting the higher order terms beyond the first degree in $\left(T - T_s\right)$, we obtain

$$T^4 = 4T_s^3 T - 3T_s^4. \tag{30}$$

Using Eqs. (28) and (30), Eqs. (26) yields:

$$\left(1 + Nr\right)\frac{\partial^2 T}{\partial y^2} + \mu\left(\frac{\partial u}{\partial y}\right)^2 + 2\left(\beta_2 + \beta_3\right)\left(\frac{\partial u}{\partial y}\right)^4 + \sigma\left(E^2 + B^2u^2 - 2EBu\right) = 0 \tag{31}$$

where $N_r = \dfrac{K^*K_{th}}{4\sigma^*\bar{T}_s^3}$ is the radiation parameter

Introducing a dimensionless temperature T^* as:

$$T^* = \frac{T_s - T}{T_s - T_m}, \tag{32}$$

where T_m is the mean tempreture and T_s is the surface temperatures.

Using Eqs. (32) and (16), we obtained the dimensionless energy equation as:

$$\left(1 + Nr\right)\frac{\partial^2 T}{\partial y^2} + \gamma_1\left(\frac{\partial u}{\partial y}\right)^2 + 2\Lambda\gamma_1\left(\frac{\partial u}{\partial y}\right)^4 + \gamma_1 Ha^2u^2 - \gamma_2 u + \gamma_3 = 0, \tag{33}$$

where $\gamma_1 = \dfrac{\mu\nu^2}{h^2 K_{th}\left(T_m - T_s\right)}$ is the Brinkman number which measure the ratio of heat produced by viscous dissipation to heat transported by molecular conduction, $\gamma_2 = \dfrac{\nu h\left(2\sigma EB + M\right)}{K_{th}\left(T_m - T_s\right)}$ is the ratio of heat generated by the interaction of the electrical and magnetic fields to heat conduction and $\gamma_3 = \dfrac{\sigma h^2 E^2}{K_{th}\left(T_m - T_s\right)}$ is the ratio of Joule heating to heat conduction.

The corresponding boundary conditions of the dimensionless energy equation are

$$T(y) = 0; y = \pm 1. \tag{34}$$

3.1. Analytical solution of temperature

Following the same procedure as for obtaining the velocity profile, the temperature profile can be achieved similarly. Here we assume the solution of the following form:

$$T = T_0 + \Lambda T_1 + ... \tag{35}$$

Inserting Eq. (35) into (33), (34) and separating at each order of Λ yields

Zero Order:

$$\left(1 + Nr\right)\frac{\partial^2 T_0}{\partial y^2} + \gamma_1\left(\frac{\partial u_0}{\partial y}\right)^2 + \gamma_1 Ha^2 u_0^2 - \gamma_2 u_0 + \gamma_3 = 0. \tag{36}$$

$$T_0\left(\pm 1\right) = 0. \tag{37}$$

Fist Order:

$$\left(1 + Nr\right)\frac{\partial^2 T_1}{\partial y^2} + \gamma_1\left(\frac{\partial u_1}{\partial y}\right)^2 + 2\Lambda\gamma_1\left(\frac{\partial u_1}{\partial y}\right)^4 + \gamma_1 Ha^2 u_1^2 - \gamma_2 u_1 = 0, \tag{38}$$

$$T_1(\pm 1) = 0. \tag{39}$$

With the solutions (24)-(25) known then (36)-(39) can be elegantly solved. MATHEMATICA software has been applied to sove Eqs. (36)-(39). The huge size of the solution suggests that only graphical solutions can be presented as shown in Figures 7–10.

4. Results and discussions

In this section, we present graphically the numerical results computed for fluid velocity and temperature distribution in the cases of porosity and radiation effects. A detailed discussion regarding the results analyzed in this investigation is provided. The results for

the steady velocities in the case of EMH flow are shown in Figures 2-4 and for the temperature distribution are displayed in Figures 5-10.

Figure 2 illustrates the influence of permeability parameter K on the velocity profiles for fixed electric H, Hartmann number Ha and constant pressure P when micro-channel shows small and large values of K. It is observed that for small values of K, the horizontal velocity increases with an increase in K. A similar behavior was also expected when K is large, because an increase in the permeability of the porous medium reduces the drag force, which tends to enhance the magnitude of the horizontal velocity. Figure 3 shows the influences of constant pressure gradient P on the velocity profiles for fixed electrokinetic parameter H, magnetic parameter Ha when micro-channel shows small and large values of K. It is noted that for small and large values of P, the horizontal velocity increases with an increase in P in the boundary layer region. Thus, increasing the constant pressure gradient in the boundary layer region yields an effect same to that of the permeability of the porous medium.

Figure 4 exhibits the influences of the dimensionless electrical strength parameter H ($H = 0.5, 1.0, 1.5$) on velocity profile when $Ha = 1, P = 1, L = 0.01$, for the cases of small permeability ($K = 0.01$) and large permeability ($K = 1$). It should be observed that an increase in velocity occurs with an increase in electrical field strength parameter H for both small and large values of K. This is due to fact that larger electrical field strength parameter H produces larger aiding force in Eq.(9) and gives rise to larger EMHD velocity in Figure 4. It is observed from Figure 5 that fluid velocity decreases on increasing the Hartmann number Ha in the boundary layer region. This is because that magnetic field decelerates fluid velocity for both small and large values of K. This is due to fact that the application of magnetic field to an electrically conducting fluid produces a resistive force called a Lorentz force. So, the higher the values of Ha, the more prominent is the reduction in velocity in the boundary layer region. Thus, increasing the electrical strength parameter H yields an effect opposite to that of the Hartmann number Ha.

Figure 6 describes the effects of non-Newtonian viscoelastic parameter Λ ($\Lambda = 0, 0.01, 0.03$) on the fluid velocity profile for the cases of small permeability ($K = 0.01$) and large permeability ($K = 1$) when $Ha = 1, H = 2, P = 1$, for the cases of small permeability ($K = 0.01$) and large permeability ($K = 1$). The non-Newtonian property of the fluid decreases with increasing Λ. From this figure, we can compare the velocity of the third-grade fluid with the velocity corresponding to the non-Newtonian second-grade fluid ($\Lambda = 0$). For

the large and small values of K, the second-grade non-Newtonian fluid flows faster than the third-grade fluid. This is due to the fact that the viscosity of third-grade fluids depending on the non-Newtonian parameter increases with Λ.

Figure 7 demonstrates the influences of radiation on fluid temperature when $Ha = 1, H = 2, P = 1, \gamma_1 = 0.01, \gamma_2 = 0.2, \gamma_3 = 0.2, L = 0.01$,and $K = 0.1$ for the cases of small values of Nr and large values of Nr. It is observed from Fig. 7 that fluid temperature increases on increasing radiation parameter Nr in the boundary layer region which implies that radiation tends to enhance fluid temperature. Figure 8 exhibits the influences of the dimensionless electrical strength parameter H (0.5, 1.0, and 1.5) on temperature profile. It should be observed that an increase in temperature occurs with an increase in electrical field strength parameter H. This behavior is similar in the case of fluid velocity. Furthermore, the larger EMHD velocity enhances the advection heat transfer, thereby reducing the local temperature but thereafter, the magnitude of the term becomes larger than the magnitude of the term. Finally, larger dimensionless temperature can be produced with the temperature profiles as in Fig. 8.

The effects of Hartmann number Ha (0.5, 1.5, and 2.5) on the temperature profiles are shown in Figure 9. From this picture, it can be found that magnetic field strength (Ha) contributes to slow down the temperature and the maximum temperature can be obtained near the center of the microchannel. This due to the fact that the Lorentz force is produced in axial direction. Therefore, the reduced flow velocity reduces the advection transport of thermal energy from the channel walls to the fluid, thereafter, the local temperature rises whereas the magnitude of the term becomes smaller than the magnitude of the term. Thus, the dimensionless temperature decreases obviously with Ha. Figure 10 illustrates the effect of the Brinkman number $\gamma_1(0.05, 0.1, 0.2)$ on the temperature through the microchannel. It is observed that the value of Brinkman number has an accelerating effect on the dimensionless temperature. The reason is that the viscous dissipation behaves like an energy source increasing the temperature of the fluid especially near the walls.

5. Conclusions

The main focus of the present investigation was to determine the analytical solutions for the problem of steady EMH micro-pump of third grade fluid flow and heat transfer through a porous micro-channel with thermal radiation and magnetic field effects. The expressions of

velocity and temperature distribution are obtained in series forms under the assumption that the non-Newtonian viscoelastic parameter has small values. The present solutions are more general and the existing solutions in the literature appear as the limiting cases. Furthermore, flow and heat transfer results for a range of values of the pertinent parameters have been reported. The significant findings are summarized below:

- with increasing the Hartmann number Ha causes Lorenz force to increase and leads to a substantial suppression of the convection, then the velocity and temperature decrease for given values of K, Λ and H.
- the permeability of the porous medium K shows opposite behavior to that of the Hartmann number in the boundary layer region.
- for small and large values of permeability of the porous medium K, the fluid velocity increases in the boundary layer region.
- increasing the constant pressure gradient P in the boundary layer region yields an effect same to that of the permeability of the porous medium K.
- with increasing the dimensionless electrical strength H yields the increase of the velocity and temperature distributions.
- increasing the electrical strength parameter H yields an effect opposite to that of the Hartmann number Ha.
- for large and small values of K, the second-grade non-Newtonian fluid flows faster than the third-grade non-Newtonian fluid.
- The fluid velocity and temperature distribution are found to decrease with the increasing third-grade parameter and attains maximum value when the fluid is of second grade ($\Lambda = 0$).

References

[1] S.O. Adesanya, J. Falade, Thermodynamics analysis of hydromagnetic third grade fluid flow through a channel filled with porous medium, Alexandria Engineering Journal 54 (2015) 615–622.

[2] M. Ayub, A. Rasheed, T. Hayat, Exact flow of a third grade fluid past a porous plate using homotopy analysis method, International Journal of Engineering Science 41 (2003) 2091–2103.

[3] T. Aziz, F. Mahomed, A. Aziz, Group invariant solutions for the unsteady mhd flow of a third grade fluid in a porous medium, International Journal of Non-Linear Mechanics 47 (2012) 792–798.

[4] R. Chakraborty, R. Dey, S. Chakraborty, Thermal characteristics of electromagnetohydrodynamic flows in narrow channels with viscous dissipation and joule heating under constant wall heat flux, International Journal of Heat and Mass Transfer 67 (2013) 1151–1162.

[5] R. Ellahi, S. Afzal, Effects of variable viscosity in a third grade fluid with porous medium: an analytic solution, Communications in Nonlinear Science and Numerical Simulation 14 (2009) 2056–2072.

[6] M. Hatami, J. Hatami, D.D. Ganji, Computer simulation of mhd blood conveying gold nanoparticles as a third grade non-newtonian nanofluid in a hollow porous vessel, Computer methods and programs in biomedicine 113 (2014) 632–641.

[7] T. Hayat, T. Javed, M. Sajid, Analytic solution for rotating flow and heat transfer analysis of a third-grade fluid, Acta Mechanica 191 (2007) 219–229.

[8] Y. Jian, D. Si, L. Chang, Q. Liu, Transient rotating electromagnetohydrodynamic micropumps between two infinite microparallel plates, Chemical Engineering Science 134 (2015) 12–22.

[9] H.J. Ko, G.S. Dulikravich, Non-reflective boundary conditions for a consistent two-dimensional planar electro-magneto-hydrodynamic flow model, in: Forum on Functional Fluids (Rheological Flows), pp. 19–23.

[10] I. Mirza, M. Abdulhameed, D. Vieru, S. Shafie, Transient electro-magneto-hydrodynamic two-phase blood flow and thermal transport through a capillary vessel, Computer Methods and Programs in Biomedicine 137 (2016) 149–166.

[11] H.B. Rokni, D.M. Alsaad, P. Valipour, Electrohydrodynamic nanofluid flow and heat transfer between two plates, Journal of Molecular Liquids 216 (2016) 583–589.

[12] A. Siddiqui, R. Mahmood, Q. Ghori, Thin film flow of a third grade fluid on a moving belt by he's homotopy perturbation method, International Journal of Nonlinear Sciences and Numerical Simulation 7 (2006) 7–14.

[13] A. Sinha, G. Shit, Electromagnetohydrodynamic flow of blood and heat transfer in a capillary with thermal radiation, Journal of Magnetism and Magnetic Materials 378 (2015) 143–151.

[14] L. Wang, Y. Jian, Q. Liu, F. Li, L. Chang, Electromagnetohydrodynamic flow and heat transfer of third grade fluids between two micro-parallel plates, Colloids and Surfaces A: Physicochemical and Engineering Aspects 494 (2016) 87–94.

[15] G. Zhao, Y. Jian, F. Li, Streaming potential and heat transfer of nanofluids in microchannels in the presence of magnetic field, Journal of Magnetism and Magnetic Materials 407 (2016) 75–82.

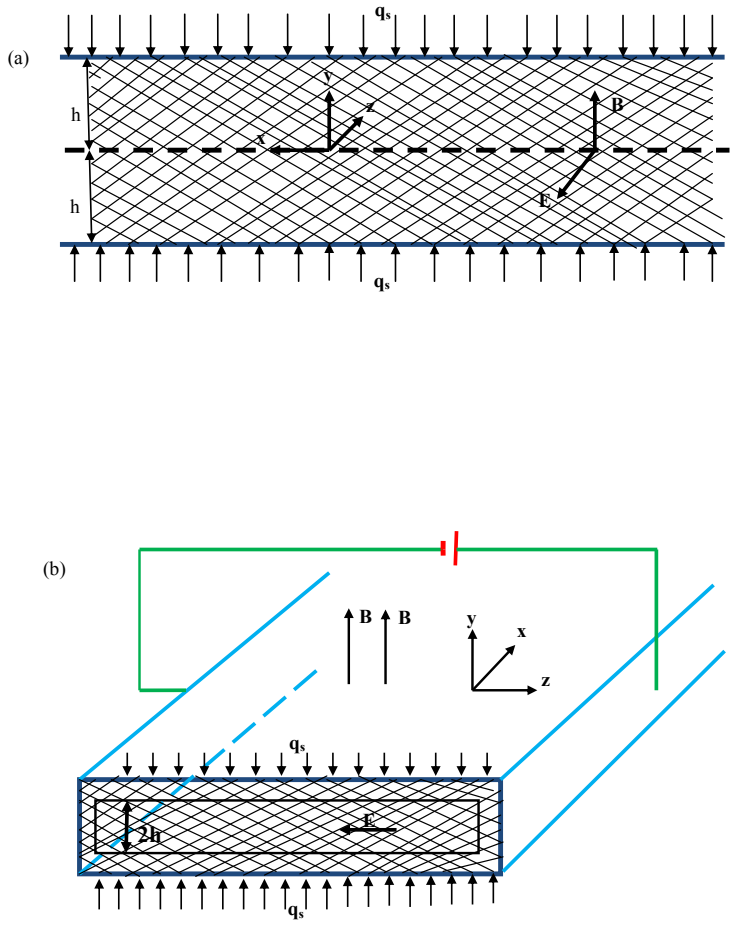

Figure 1: Schematic of the physical modeling of EMHD micro-pump through a porous micro-channel, (a) 3D view of the EMHD micro-pump, (b) Duct's crosssection of the EMHD micro-pump

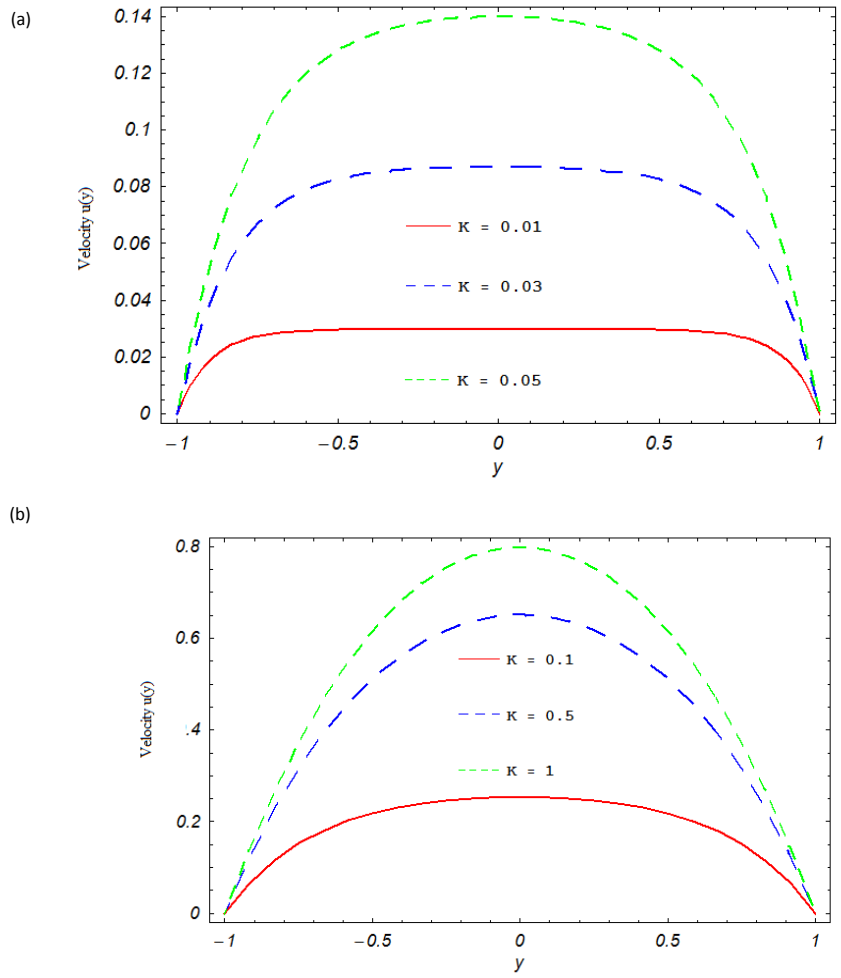

.

Figure 2: Velocity profiles with different values of permeability of a porous medium K when $Ha = 1, H = 2, P = 1$, for the case (a) small values of K (b) large values of K

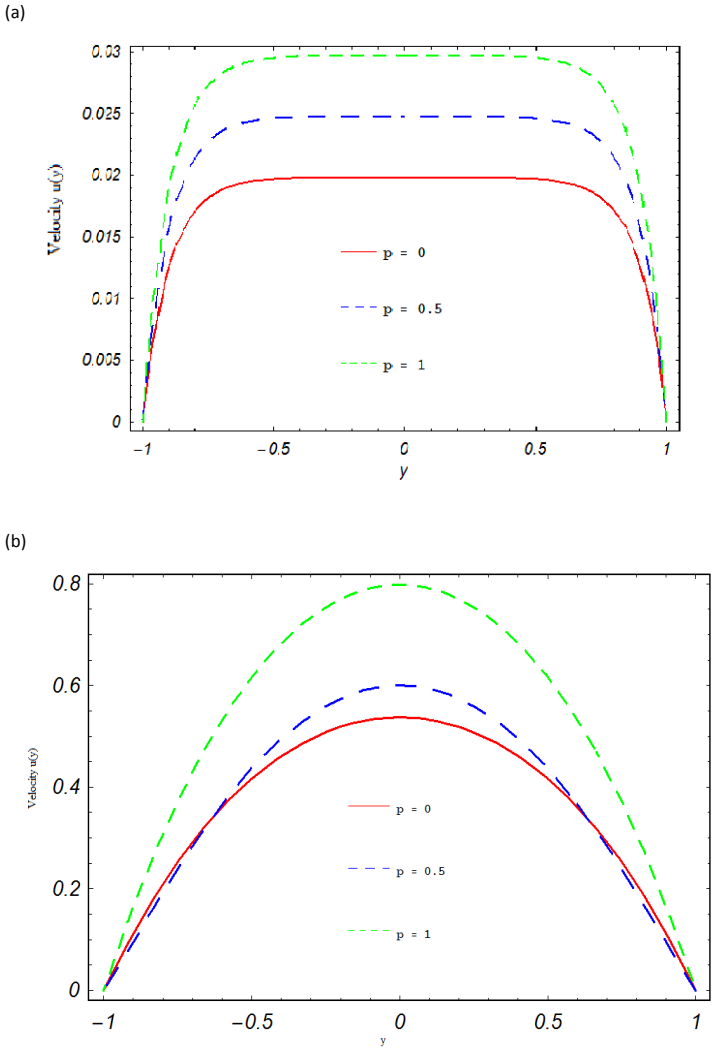

Figure 3: Velocity profiles with different values of constant pressure P when $Ha = 1, H = 2, \Lambda = 0.01$, for the case (a) small permeability ($K = 0.01$) (b) large permeability ($K = 1$)

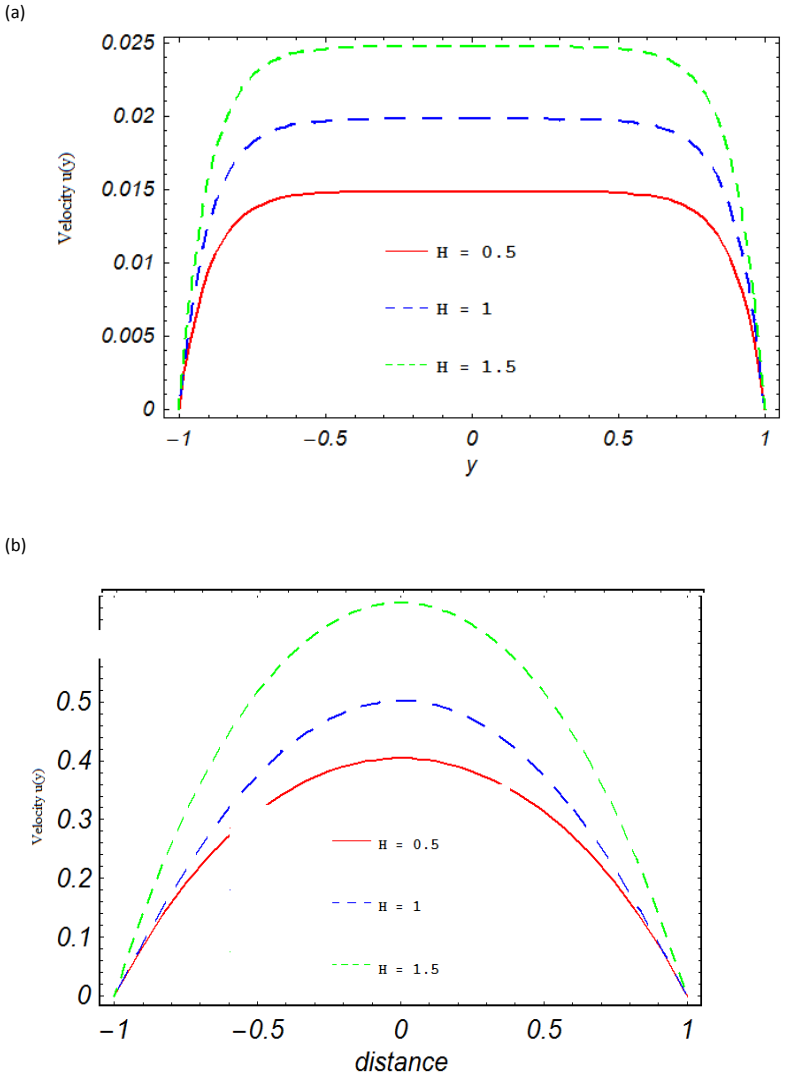

Figure 4: Velocity profiles with differen values of electrical strength parameter H when $Ha = 1, P = 1$, $\Lambda = 0.01$ for the case (a) small permeability ($K = 0.01$) (b) large permeability ($K = 1$)

(a)

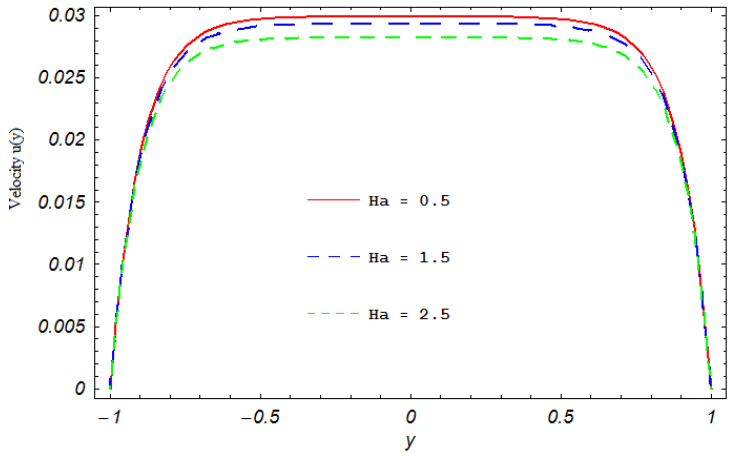

(b)

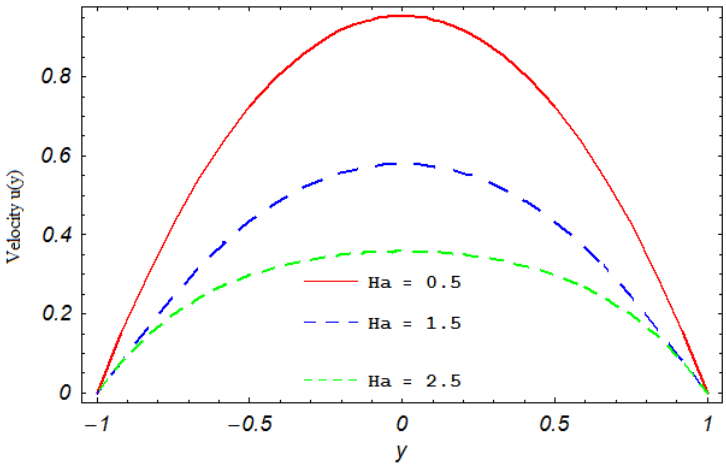

Figure 5: Velocity profiles with different values of Hartmann number Ha when $P = 1, H = 2$, $\Lambda = 0.01$, for the case (a) small permeability ($K = 0.01$) (b) large permeability ($K = 1$)

(a)

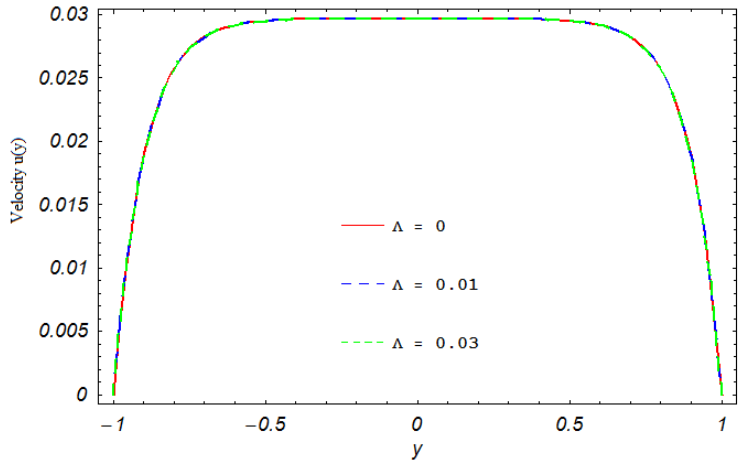

(b)

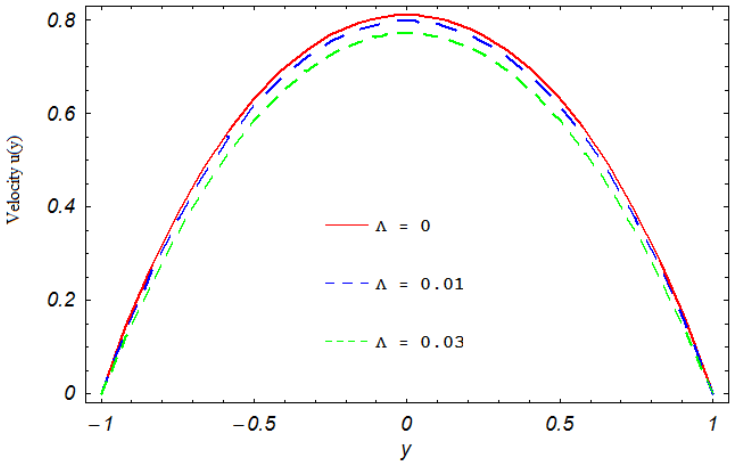

Figure 6: Velocity profiles with different values of different non-Newtonian parameter Λ when $Ha = 1, H = 2, P = 1$, for the case (a) small permeability ($K = 0.01$) (b) large permeability ($K = 1$)

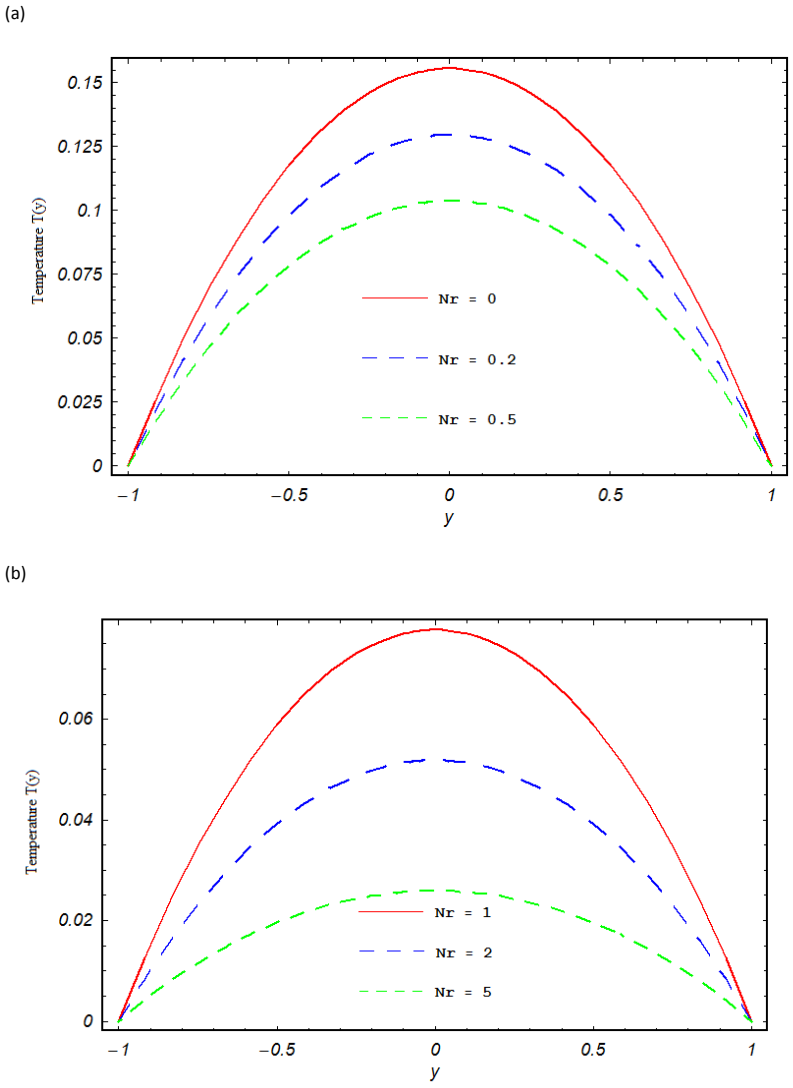

Figure 7: Temperature profiles with different values of thermal radiation when $Ha = 1, H = 2, P = 1, \gamma_1 = 0.01, \gamma_2 = 0.2, \gamma_3 = 0.2, \Lambda = 0.01$, and $K = 0.1$ for the case (a) small values of Nr (b) large values of Nr

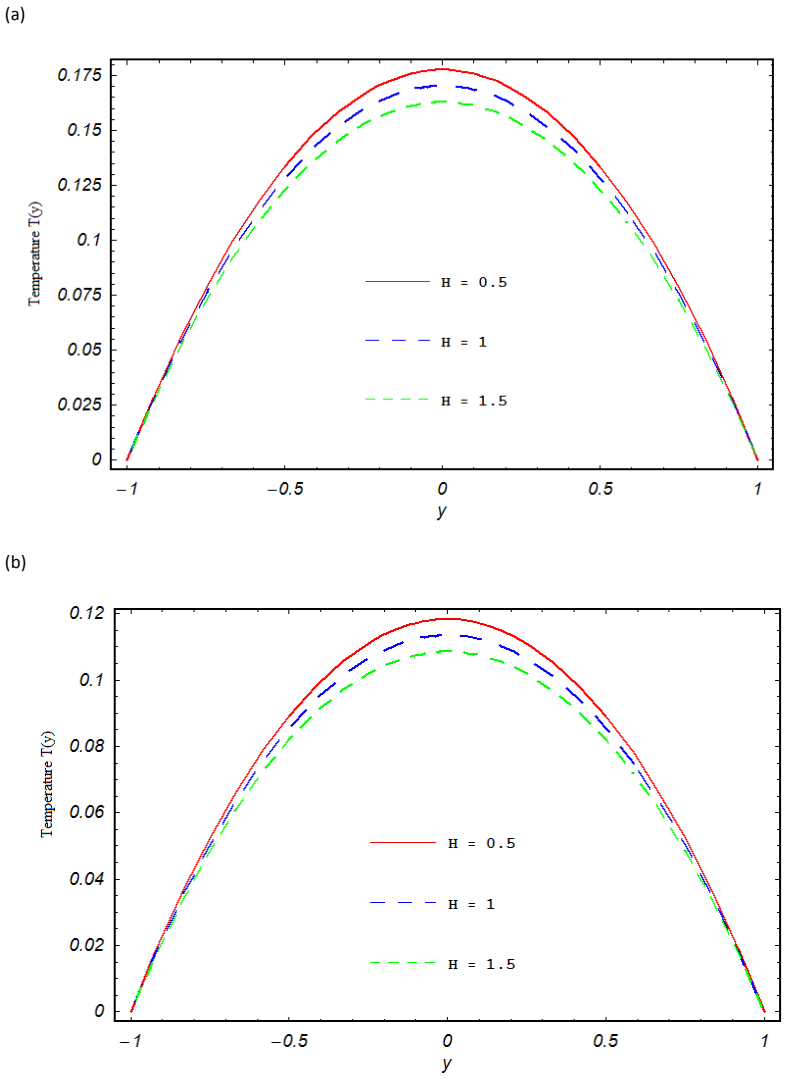

Figure 8: Temperature profiles with different values of Hartmann number Ha when $Ha = 1$, $P = 1$, $\gamma_1 = 0.01, \gamma_2 = 0.2, \gamma_3 = 0.2, \Lambda = 0.01$, for the case (a) without thermal radiation ($Nr = 0$) (b) with thermal radiation ($Nr = 0.5$)

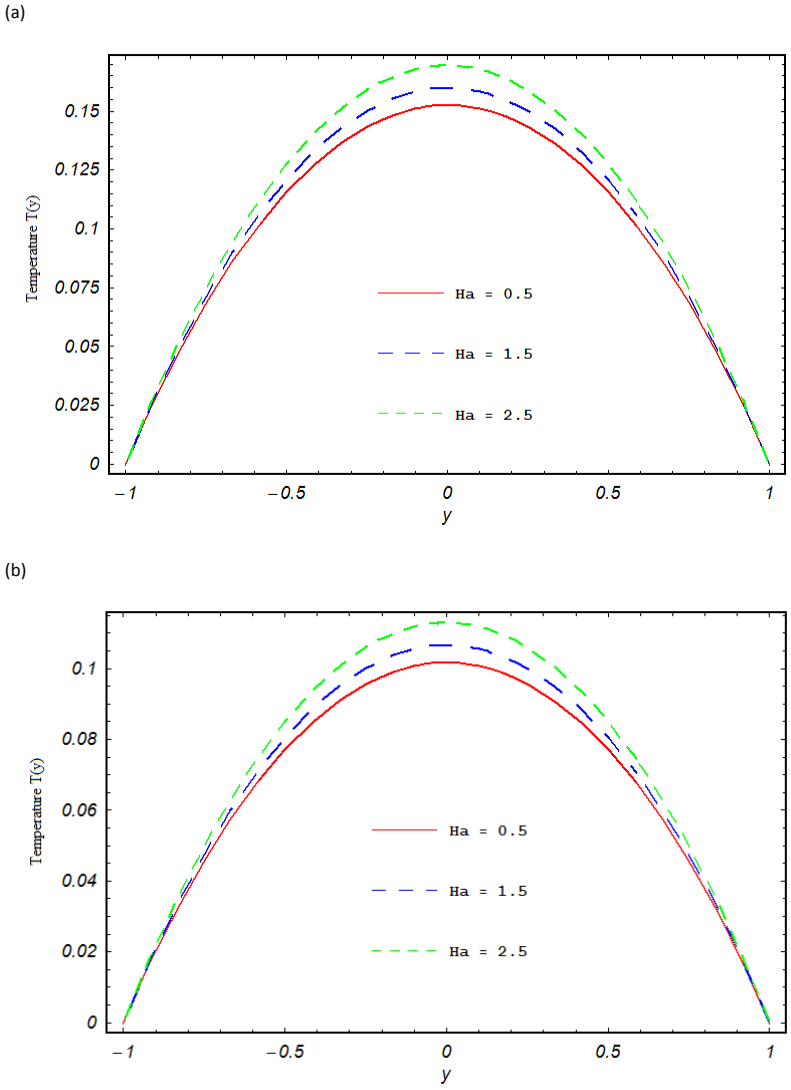

Figure 9: Temperature profiles with different values of electrical strength parameter H when $H = 2, P = 1, \gamma_1 = 0.01, \gamma_2 = 0.2, \gamma_3 = 0.2, \Lambda = 0.01$, for the case (a) without thermal radiation ($Nr = 0$) (b) with thermal radiation ($Nr = 0.5$)

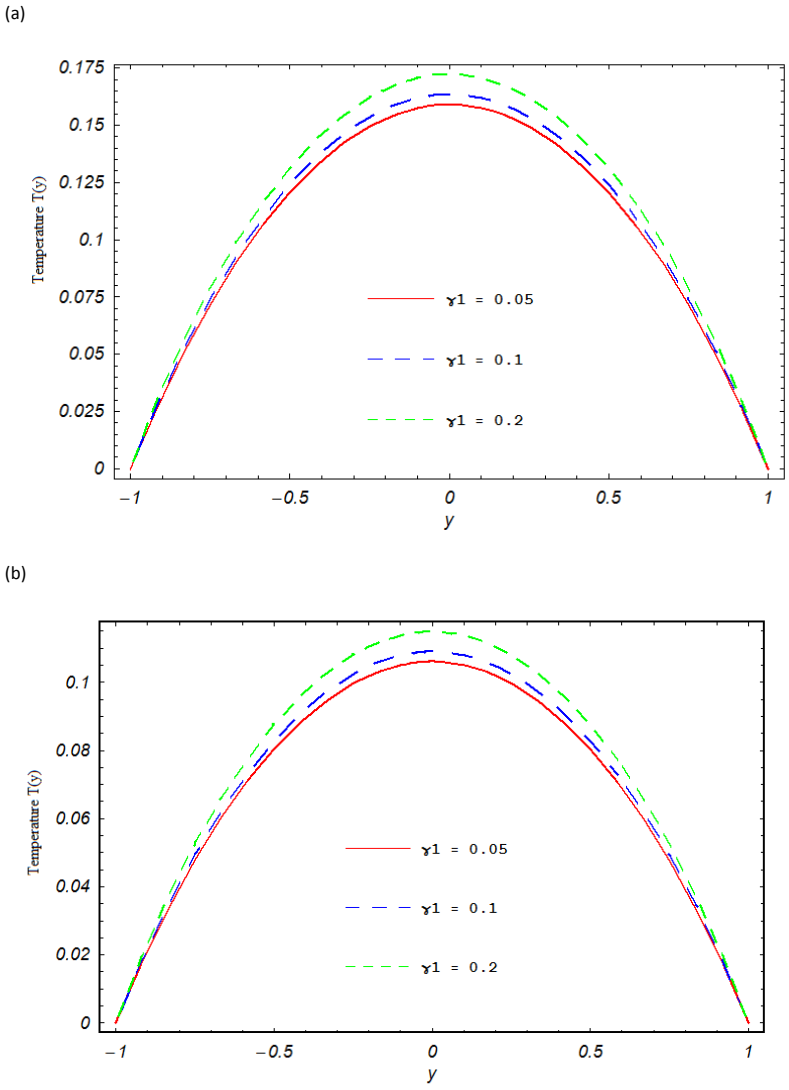

Figure 10: Temperature profiles with different values of Brinkman number γ_1 when Ha=1,$H = 2, P = 1, \gamma_2 = 0.2, \gamma_3 = 0.2, \Lambda = 0.01$, for the case (a) without thermal radiation ($Nr = 0$) (b) with thermal radiation ($Nr = 0.5$)